# MICRO-FRACTURE MAPS IN PROGRESSIVELY DRAWN PEARLITIC STEELS UNDER TRIAXIAL STRESS STATES

**F. J. Ayaso and J. Toribio**
**Department of Materials Engineering, University of Salamanca**
**E.P.S., Campus Viriato, Avda. Requejo 33, 49022 Zamora**
**Tel: 980 545 000; Fax: 980 545 002, E-mail: toribio@usal.es**

**Abstract.** In this paper the fracture performance of axisymmetric notched samples taken from prestressing steels with different levels of cold drawing is studied. Fractographic analysis of the samples by means of scanning electron microscope (SEM) revealed the microscopic topographies after failure and allowed the assembly of micro-fracture maps (MFM) covering the whole fracture surface and containing relevant information on the micromechanisms of fracture in the material. With regard to the influence of the stress triaxiality (constraint), the behaviour is more ductile in the case of blunt notches than in the case of sharp notches. In the matter of the influence of the cold drawing degree, the fracture behaviour becomes more ductile as the strain hardening level of the steel increases, so that cleavage is predominant in the fracture area of slightly drawn steels, whereas the presence of micro-void coalescence (MVC) increases with the degree of cold drawing and becomes predominant in the case of the most heavily drawn steels in which cleavage can hardly be detected as an extended region.

**Resumen.** En este artículo se estudia el comportamiento en fractura de muestras axisimétricas entalladas tomadas de alambres de acero de pretensado con distinto grado de trefilado. El análisis fractográfico de las muestras por medio de microscopía electrónica de barrido (MEB) reveló las topografías microscópicas de fractura y permitió el ensamblaje de mapas de fractura microscópica (MFM) cubriendo toda la superficie de rotura y conteniendo información relevante acerca de los micromecanismos de fractura en el material. Con respecto a la influencia de la triaxialidad tensional (constreñimiento), el comportamiento de los alambres es más dúctil en el caso de entallas romas que en el caso de entallas afiladas. En lo que se refiere a la influencia del grado de trefilado, el comportamiento en fractura se hace más dúctil a medida que el nivel de endurecimiento por deformación aumenta, de modo que el clivaje es predominante en aceros débilmente trefilados, mientras que la presencia de zonas creadas por coalescencia de microhuecos (CMH) aumenta con el grado de trefilado y llega a ser predominante en aceros fuertemente trefilados en los cuales apenas se detecta fractura por clivaje.

## 1. INTRODUCTION

Cold drawn eutectoid steels are structural materials of the greatest interest in civil engineering because they are frequently used in the form of wires and cables in prestressed concrete which usually works under very high stress levels and surrounded by harsh environments. The manufacturing process consists of cold drawing a previously hot rolled bar in order to increase the yield strength by means of a strain hardening mechanism.

Such a heavy drawing (with its associated plastic deformation) produces important microstructural changes in the steels [1-3] so that their macroscopic characteristics are seriously affected. As the final aim of manufacturing, classical mechanical properties such as the yield strength and the ultimate tensile stress are improved with cold drawing. In addition to this, microstructural changes also affect (in a less clear manner) the fracture behaviour in air and in aggressive environments [4-10], and the consequences are far from being totally understood.

This paper analyzes the fracture process in axisymmetric notched samples of high strength pearlitic steel governed by two key variables: the *stress triaxiality* in the vicinity of the notch tip (produced by notches of very different depths and radii) and the *yield strength* of the material (controlled by the degree of cold drawing achieved during the manufacturing process to make prestressing steel for civil engineering). The final aim of this research work is the assembly of micro-fracture maps (MFM) covering the whole fracture surface and containing relevant information on the micro-mechanisms of fracture in the material.

## 2. EXPERIMENTAL PROGRAMME

Samples from a real manufacturing process were supplied by EMESA TREFILERIA. The manufacture chain was stopped in the course of the process, and samples of five intermediate stages were extracted, apart from the original material or base product (hot rolled bar: not cold drawn at all) and the final commercial product (prestressing steel wire: heavily cold drawn). Thus the *drawing intensity* (straining level) is treated as the fundamental variable to elucidate the consequences of manufacturing on the posterior fracture behaviour.

The different steels were named with digits 0 to 6 which indicate the number of cold drawing steps undergone. Table 1 shows the chemical composition common to all steels, and Table 2 includes the diameter ($D_i$), the cold drawing degree ($D_i/D_0$), the yield strength ($\sigma_{02}$), the ultimate tensile stress (UTS) and the fracture toughness ($K_{IC}$) of the steels.

**Table 1.** Chemical composition of the steels

| C | Mn | Si | P | S | Cr | V | Al |
|---|---|---|---|---|---|---|---|
| 0.80 | 0.69 | 0.23 | 0.012 | 0.009 | 0.265 | 0.060 | 0.004 |

**Table 2.** Diameter ($D_i$), cold drawing degree ($D_i/D_0$), yield strength ($\sigma_{02}$), ultimate tensile stress (UTS) and fracture toughness ($K_{IC}$) of the different steel wires.

| Steel | 0 | 1 | 2 | 3 | 4 | 5 | 6 |
|---|---|---|---|---|---|---|---|
| $D_i$ (mm) | 12.00 | 10.80 | 9.75 | 8.90 | 8.15 | 7.50 | 7.00 |
| $D_i/D_0$ | 1 | 0.90 | 0.81 | 0.74 | 0.68 | 0.62 | 0.58 |
| $\sigma_{02}$ (GPa) | 0.686 | 1.100 | 1.157 | 1.212 | 1.239 | 1.271 | 1.506 |
| UTS (GPa) | 1.175 | 1.294 | 1.347 | 1.509 | 1.521 | 1.526 | 1.762 |
| $K_{IC}$ (MPam$^{1/2}$) | 60.1 | 61.2 | 70.0 | 74.4 | 110.1 | 106.5 | 107.9 |

The stress-strain curves of the seven steels with increasing degree of cold drawing appear in Fig. 1, where a clear improvement of traditional mechanical properties is achieved after manufacturing, due to a strain hardening mechanism activated in the steels.

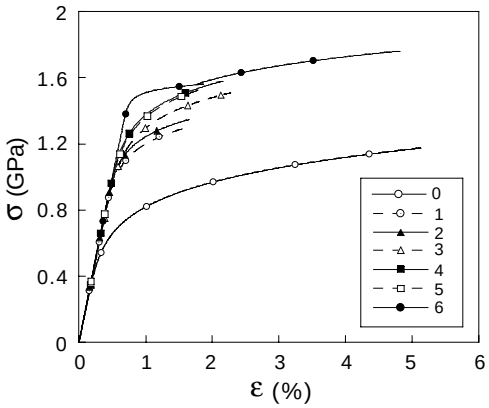


**Fig. 1.** Stress-strain curves of the different steels used in the experimental programme.

Tensile fracture tests were performed on axisymmetric notched specimens with a circumferentially-shaped notch. Four notch geometries were used with each material, in order to achieve very different stress states in the vicinity of the notch tip and thus very distinct *constraint* situations, thus allowing an analysis of the influence of such factors on the fracture processes. The dimensions of the specimens —named A, B, C and D throughout this paper— were the following:

- Geometry A : R/D = 0.03, A/D = 0.10
- Geometry B : R/D = 0.05, A/D = 0.30
- Geometry C : R/D = 0.40, A/D = 0.10
- Geometry D : R/D = 0.40, A/D = 0.30

where R is the notch radius, A the notch depth and D the external diameter of the specimen. These four notched geometries are depicted in Fig. 2. Three fracture tests were performed for each material and geometry.

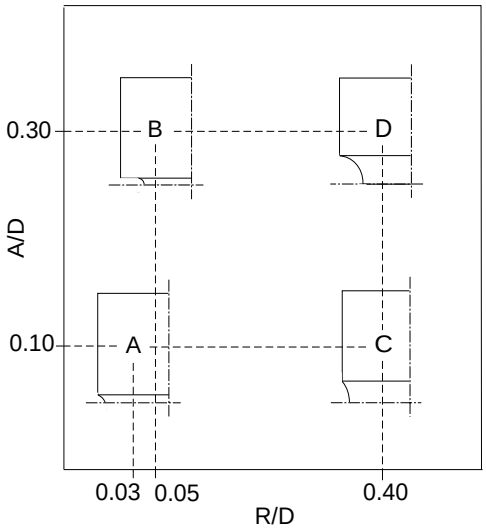


**Fig. 2.** Notched geometries used in the experiments.

## 3. MICROSCOPIC APPROACH

A fractographic study by scanning electron microscopy (SEM) was performed on the fracture surfaces after the tests. The specimens with blunt notch (geometries C and D) exhibit a central fracture area of fibrous aspect, detectable by simple visual inspection. This fibrous area is formed mainly by micro-void coalescence (MVC) with some isolated cleavage regions which can also be detected. Such a special feature will be named MVC* throughout this paper (cf. Fig. 3), and it can be considered as the fracture process zone (FPZ) in notched geometries C and D, since fracture initiates in that fibrous MVC* region and propagates in an unstable manner and radial direction by cleavage (C, shown in Fig. 4) towards the periphery of the specimens in which the external ring consists of conventional micro-void coalescence (MVC, cf. Fig. 5).

With regard to the sharp notch specimens A and B, the FPZ is located in the external ring, i.e., in the vicinity of the notch tip (due to the very high stress triaxiality levels there), and specifically in a region of the same in

which the fractographic appearance is also MVC*-type (Fig. 3). After the initiation in this area, fracture propagates by radial cleavage C (Fig. 4) emanating from the FPZ. The afore-said MVC* region in samples of geometry A really resembles those for samples of geometries C and D and it is clearly different from the rest of the external ring which finally fails by conventional MVC (Fig. 5).

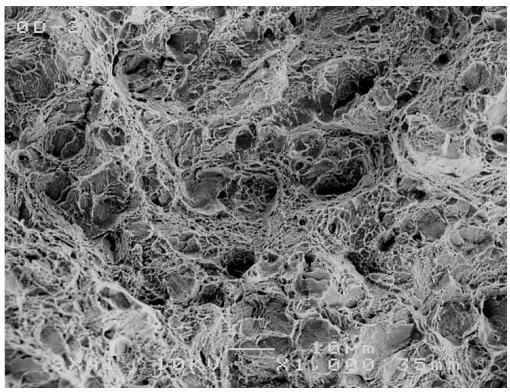

**Fig. 3.** Fibrous micro-void coalescence (MVC*).

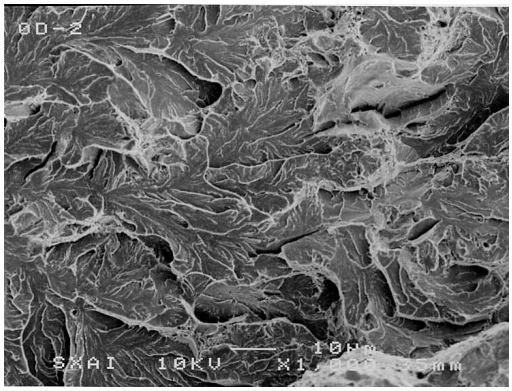

**Fig. 4.** Unstable fracture by cleavage (C).

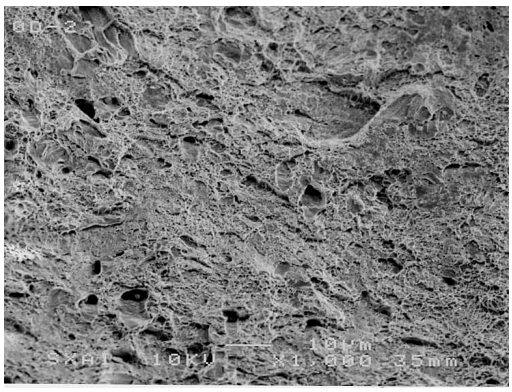

**Fig. 5.** Conventional micro-void coalescence (MVC).

Fig. 6 shows a sketch of the fracture process (initiation and propagation) in the notched specimens. The FPZ is bigger in samples with notch geometry A than in those with notch geometry B, due to the higher triaxiality level in the latter. Thus the higher the maximum stress triaxiality created by the notch, the lower the depth of the FPZ in the vicinity of the notch tip. The more elevated stress triaxiality in geometry B also explains why in this case there are several initiation sites for fracture (multiple cleavage origins) at a certain distance from the notch tip, in contrast with the single cleavage origin in geometry A. In notched geometries C and D, fracture initiates in the central fibrous MVC* region and propagates in unstable manner and radial direction by cleavage (C) towards the periphery of the specimens.

The detailed fractographic results are given in Figs. 7 to 10 in the form of micro-fracture maps (MFM) which include all the microscopic fracture. These fractographic results are fully consistent with the analysis of the FPZ performed in the previous paragraphs in the matter of the influence of the stress triaxiality (constraint) on fracture processes in the vicinity of notches, the behaviour being more ductile in the case of blunt notches than in the case of sharp notches.

With regard to the influence of the cold drawing degree, the fracture behaviour becomes more ductile as the strain hardening level of the steel increases, so that cleavage is predominant in the fracture area of slightly drawn steels, whereas the presence of MVC increases with the cold drawing degree and becomes predominant in the case of the most heavily drawn steels in which cleavage can hardly be detected as an extended region.

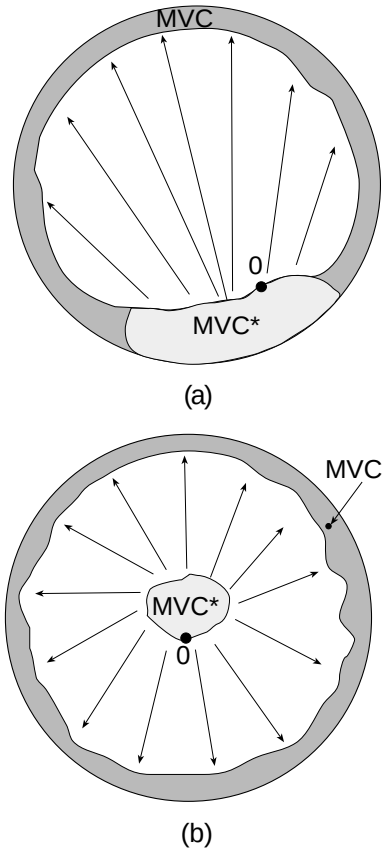


**Fig. 6.** Fracture process zone (FPZ) in the notched samples: (a) sharply notched geometries A and B; (b) bluntly notched geometries C and D.

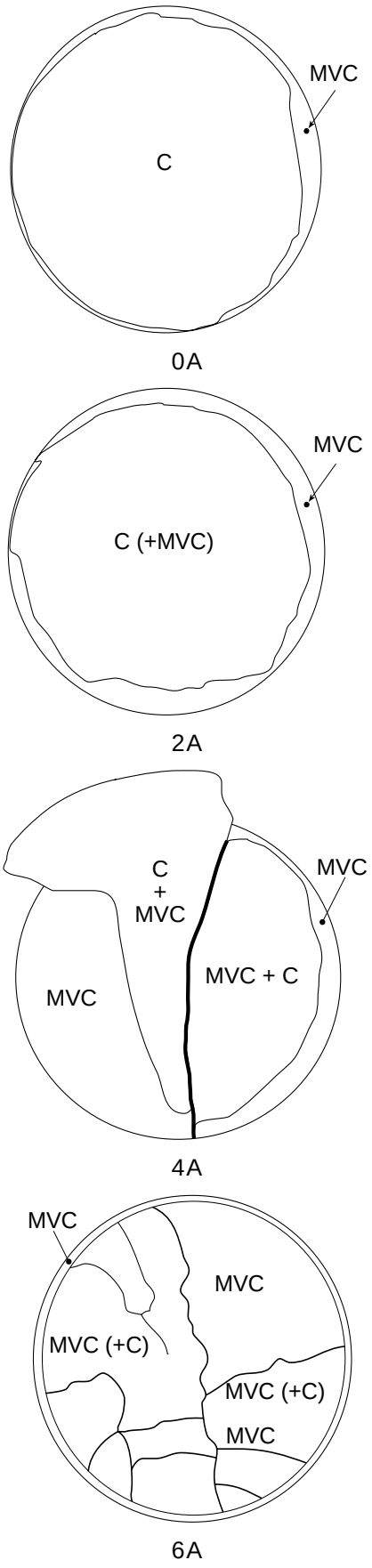


**Fig. 7.** Micro-fracture maps (MFM) in samples A.

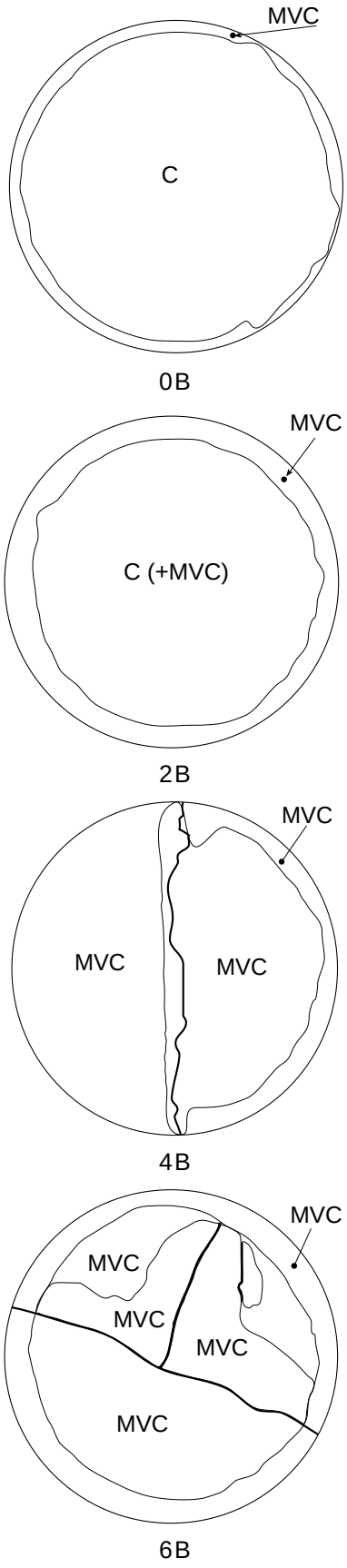


**Fig. 8.** Micro-fracture maps (MFM) in samples B.

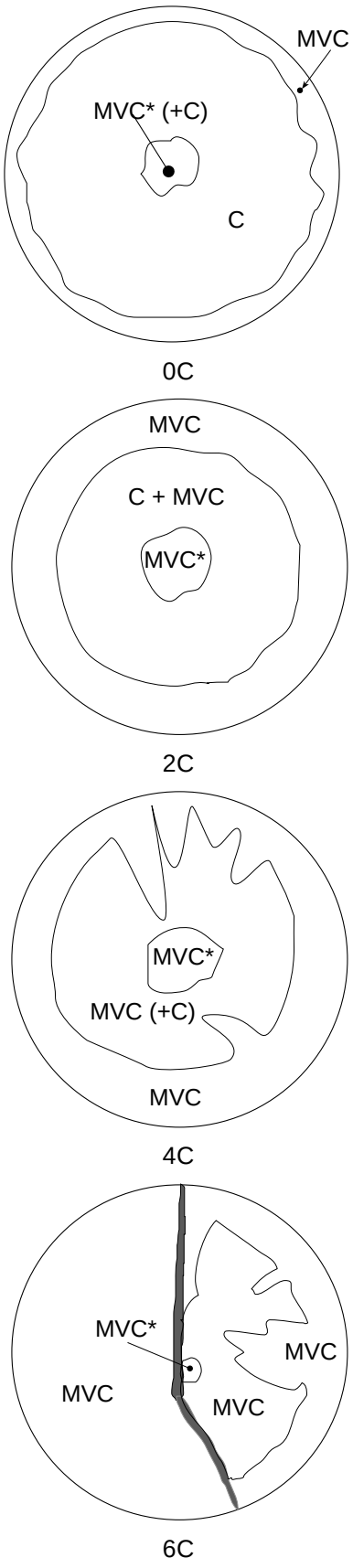


**Fig. 9.** Micro-fracture maps (MFM) in samples C.

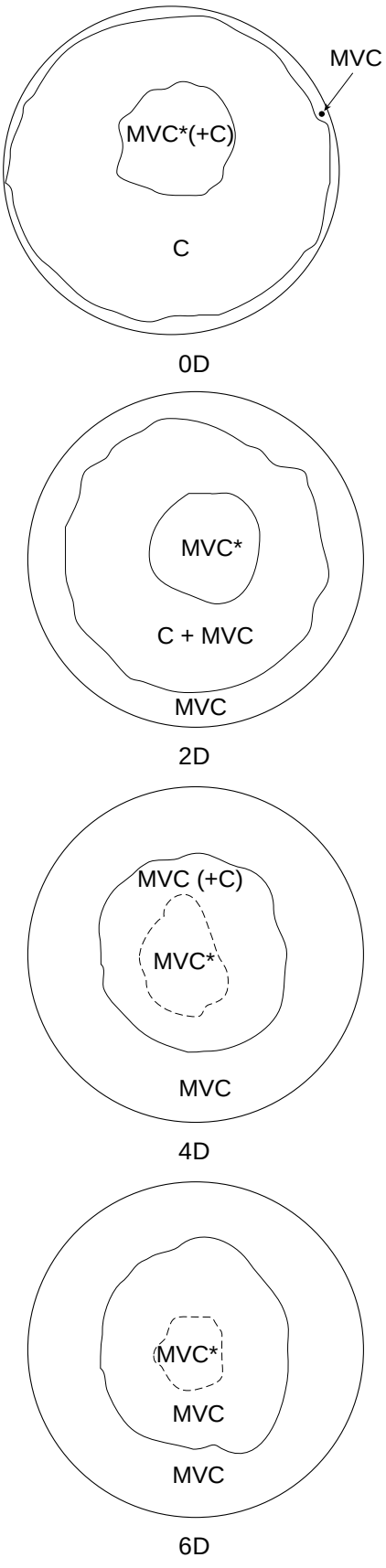


**Fig. 10.** Micro-fracture maps (MFM) in samples D.

## 4. CONCLUSIONS

The fracture micromechanisms in notched samples of progressively drawn steels were analysed in this work. The two predominant fractographic modes were ductile micro-void coalescence (MVC) and brittle cleavage. The locations and proportions of both topographies depend on the stress triaxiality (constraint) generated by the notch and on the degree of cold drawing of each steel.

Micro-fracture maps (MFM) were assembled to cover the whole fractured area and to perform a quantitative evaluation of the fractographic modes by means of image analysis techniques. As a general trend, the fracture behaviour becomes progressively more ductile (a higher proportion of the MVC mode) as the degree of cold drawing increases, but this trend is interrupted when the anisotropic fracture behaviour (with crack deflection) appears in the most heavily drawn steels.

Sharply notched geometries A and B exhibit peripheral fracture initiation from an external MVC ring (at local areas with special MVC*) and cleavage propagation towards the inner points, whereas bluntly notched geometries C and D show a central fracture initiation (fibrous zone formed by MVC*), radial cleavage propagation towards the periphery and final cup and cone fracture in the external ring.

Both the external ring in geometries A and B and the fracture core and the external ring in geometries C and D are constituted by MVC fractography, but the general features of the topography and the size of micro-voids are different from one to another. The micro-voids are bigger and the aspect more fibrous (MVC*) in the core of samples C and D and in local areas of the external ring in specimens A and B.

The above considerations allow a definition of the area in which fracture initiates or fracture process zone (FPZ) as the external ring by MVC (with local areas by MVC*) in sharp notch geometries A and B exhibitting brittle fracture behaviour, or as the central fibrous region (exclusively formed by MVC*) in blunt notch specimens C and D showing ductile fracture behaviour.

***Acknowledgments***
The financial support (Grant MAT2002-01831) of this work by the Spanish Ministry of Science and Technology (MCYT) and FEDER is gratefully acknowledged. In addition, the authors wish to express their gratitude to EMESA TREFILERIA S.A. (La Coruña, Spain) for providing the steel used in the experimental programme.

## REFERENCES

[1] Dewey, M.A.P. y Briers, G.W., "Structure of heavily cold drawn eutectoid steel*", J. Iron and Steel Inst.* **2**, 102-103 (1966).

[2] Embury, J.D. y Fisher, R.M., "The structure and properties of drawn pearlite", *Acta Metall*. **14**, 147-159 (1966).

[3] Langford, G., "A study of the deformation of patented steel wire", *Metall. Trans*. **1**, 465-477 (1970).

[4] Toledano, M. y Toribio, J., "Comportamiento en fatiga de aceros perlíticos con distinto grado de trefilado", *An. Mec. Fractura* **16**, 125-130 (1999).

[5] Toledano, M. y Toribio, J., "Influencia del proceso de fabricación sobre la tenacidad de fractura de aceros perlíticos trefilados", *An. Mec. Fractura* **15**, 419-424 (1998).

[6] Ovejero, E. y Toribio, J., "Fragilización por hidrógeno de aceros eutectoides con trefilado progresivo", *An. Mec. Fractura* **15**, 367-371 (1998).

[7] Ovejero, E. y Toribio, J., "Micromecanismos de fractura por disolución anódica localizada en aceros perlíticos trefilados", *An. Mec. Fractura* **16**, 401-406 (1999).

[8] Ayaso, F.J. y Toribio, J., "Comportamiento en fractura de alambres entallados de acero de alta resistencia: influencia del límite elástico", *An. Mec. Fractura* **18**, 295-302 (2001).

[9] Ayaso, F.J. y Toribio, J., "Micromecanismos de fractura en aceros perlíticos progresivamente trefilados", *An. Mec. Fractura* **19**, 141-146 (2002).

[10] Ayaso, F.J. y Toribio, J., "Modelización del proceso de fractura en probetas entalladas mediante el método de los elementos finitos", *An. Mec. Fractura* **19**, 385-392 (2002).